

KINETICS AND MECHANISMS FOR REMOVAL OF CIRCULATING SINGLE-STRANDED DNA IN MICE*

BY WOODRUFF EMLEN AND MART MANNIK

(From the Department of Medicine, Division of Rheumatology, the University of Washington
School of Medicine, Seattle, Washington 98195)

DNA-anti-DNA immune complexes are thought to play a major role in the pathogenesis of tissue injury in systemic lupus erythematosus (SLE)¹ (1, 2). Involved kidneys and skin contained deposits of extranuclear single-stranded DNA (ssDNA), double-stranded DNA (dsDNA) and antibodies to DNA (1, 3-5). The presence of antibodies to DNA in circulation was not sufficient to induce disease (6-8), leading several investigators to propose that DNA antigen must be present in the circulation or deposited in tissues to form immune complexes (2, 6, 9). Sera of some SLE patients contained significantly higher levels of ssDNA and dsDNA than did normal controls (2, 9-11), and serial studies on some of these patients (2, 9) indicated that serum DNA antigen and anti-DNA antibody levels may alternate, suggesting possible intermittent formation of immune complexes in the circulation. Tan (12) and Gabrielsen (13) postulated that DNA is normally released into the circulation with cell breakdown in skin and bone marrow, or with tissue injury.

The in vivo behavior and breakdown of DNA was first studied by LeDoux (14) and others (15, 16) with reference to the potential transforming ability of exogenous viral DNA. They found that DNA was rapidly degraded and that its transforming ability was destroyed in vivo within several minutes. Tsumita and Iwanaga (17) reported that >90% of administered calf thymus DNA was removed from the circulation of mice within 30 min, and that the major organ of uptake was the liver. Chused et al. (18) confirmed the rapid clearance (90% at 20 min) for both single-stranded and double-stranded KB-cell DNA and they showed that early clearance was faster in older NZB/W mice with antibodies to DNA than in younger mice without detectable antibodies to DNA. Furthermore, DNA appeared to be removed as an intact macromolecule, and reticuloendothelial uptake was thought to be the mechanism responsible. Natali and Tan (19), using native calf thymus DNA in rabbits, and Dorsch et al. (20) and Chia et al. (21), using denatured calf thymus DNA in mice, confirmed the rapid clearance of DNA from circulation.

This rapid clearance of DNA in experimental animals appears inconsistent with the finding of high levels (up to 200 $\mu\text{g}/\text{ml}$) of circulating DNA in patients with SLE (9). This would suggest that under some conditions, the DNA removal mechanism is altered, that the DNA itself is different, or that large amounts of DNA are released into

* Supported by research grant AM11476 from the National Institute of Arthritis, Metabolism and Digestive Diseases.

¹ Abbreviations used in this paper: dsDNA, double-stranded deoxyribonucleic acid; K_m , Michaelis-Menten constant; PAGE, polyacrylamide gel electrophoresis; PBS, phosphate-buffered saline; SLE, systemic lupus erythematosus; ssDNA, single-stranded deoxyribonucleic acid; TCA, trichloroacetic acid; V_m , maximum velocity.

circulation. Previous clearance studies in animals (18–20) employed only one or several low doses of DNA, well below the measured concentrations in SLE patients.

For these reasons, ssDNA clearance kinetics were examined using a variety of doses of a defined preparation. The data indicate that ssDNA clearance mechanisms are saturable at relatively low doses of ssDNA, and that a hepatic membrane-bound enzyme, as well as circulating endonucleases, contributes to the removal and degradation of circulating ssDNA.

Materials and Methods

Preparation and Iodination of DNA. Calf thymus DNA (Lot 36E672; Worthington Biochemical Corp., Freehold, N. J.) was dissolved to a concentration of 1 mg/ml in 0.003 M NaCl, passed through an HAWP 2500 Millipore filter (Millipore Corp., Bedford, Mass.), and stored at 4°C. 5-ml aliquots were denatured by placing them in a boiling water bath for 60 min, followed by rapid cooling on ice. This heat-denatured DNA solution was mixed with hydroxyapatite (DNA-grade Bio-Gel HTP; Bio-Rad Laboratories, Richmond, Calif.) at 1 mg DNA/g of hydroxyapatite and washed serially with 0.08 M, 0.16 M, and 0.48 M sodium phosphate buffer at pH 6.8, according to the method of Paetkau and Langman (22). The DNA recovered with 0.16 M sodium phosphate was considered ssDNA (23). To assess the amount of contamination with dsDNA, *Neurospora crassa* single-stranded endonuclease (Miles Laboratories Inc., Elkhart, Ind.) was added at 30 U/ μ g, and the mixture was incubated for 60 min at 37°C. 91% of the DNA was hydrolyzed to trichloroacetic acid (TCA)-soluble products, indicating <10% double-stranded material in the ssDNA preparation. ssDNA was filtered over Sepharose 4B columns (Pharmacia Fine Chemicals, Piscataway, N. J.) in 0.2 M sodium borate and 0.15 M NaCl at pH 8.0. The elution pattern was recorded by absorbance at 260 nm and it revealed a large excluded peak representing 40–50% of the initial preparation, as well as a broader included peak. In an attempt to obtain a relatively large molecular weight, but a homogenous preparation, the fractions in the ascending portion and peak of the included curve were pooled (designated as ssDNA Pool II), characterized, and used in subsequent animal studies.

When iodinated ssDNA was needed, the ssDNA eluted from hydroxyapatite with 0.16 M sodium phosphate was labeled with ^{125}I , according to the method of Commerford (24). Adequate labeling was obtained, with specific activities in the range of 5×10^4 – 10^5 cpm/ μ g. After extensive dialyses to remove free ^{125}I , preparations were subjected to gel filtration, as described above. The elution pattern was found to be the same as that of unlabeled DNA, and the same fractions from the included peak were pooled (^{125}I -ssDNA Pool II) for use in animal experiments.

To insure that the ^{125}I had been incorporated into DNA rather than into contaminating protein or RNA, the ^{125}I -ssDNA was incubated with 100 μ g protease/ μ g DNA (Protease Type VII, Sigma Chemical Co., St. Louis, Mo.) or with 100 μ g RNase/ μ g DNA (RNase I, Miles Laboratories Inc.), at 37°C for 24 h, and the amount of ^{125}I -labeled soluble in 10% TCA was determined to indicate the presence of labeled amino acids or ribonucleotides. Before enzyme treatment, 1.5–2.0% of the ^{125}I -ssDNA was soluble, and was believed to represent free ^{125}I or ^{125}I -deoxycytidine contamination. Treatment with protease failed to release any additional soluble label. RNase treatment increased the soluble products from 2 to 3%. We therefore concluded that the ^{125}I -ssDNA preparations were contaminated with \approx 1% RNA, and no measurable protein. Treatment with protease and/or RNase was therefore not performed on the preparations used in animal experiments.

Determination of DNA Size. Electrophoresis of ssDNA samples was performed in a 3.5% polyacrylamide gel, according to the method of Maniatis et al. (25), using bromophenol blue and xylene cyanol as markers. Electrophoresis was performed on a 9 \times 9-cm gel slab, 2–3 mm thick, at a voltage of 15 V/cm for 2–3 h. Gels were cut into 3-mm slices, counted for radioactivity, and the distance migrated for each peak was expressed as a fraction of the bromophenol blue migration. Using the standard curves of Maniatis et al., obtained with ϕ X 174 ssDNA fragments (25), the mean size of the ssDNA (Pool II) was estimated to be 450 nucleotides, with less than 5% smaller than 100 or greater than 1,000 nucleotides. Plasma samples, obtained in heparin-coated micropipettes at varying intervals after injection of radiolabeled ssDNA preparation, were diluted to 80 μ l with

0.01 M phosphate-buffered saline (PBS) at pH 7.2 and then examined under the same conditions of electrophoresis.

Animal Experiments. Female 3- to 4-month-old C57Bl/6J mice (18–22 g) were given potassium iodide in their drinking water at least 12 h before experiments. Pool II ssDNA and Pool II ¹²⁵I-ssDNA were combined to obtain the desired dose and radioactivity for injection. Control experiments in which the clearance kinetics of labeled DNA were compared to the clearance kinetics of a mixture of labeled and unlabeled DNA revealed no differences in in vivo behavior of the two preparations.

Varying doses of ssDNA (2, 10, 50, 100, and 500 μ g) in a 0.5-ml volume of borate buffer were injected into the tail vein, and 20- μ l blood samples were obtained from the retro-orbital venous plexus at 30 s, 1, 2, 3, 5, 10, 20, 30, and 40 min, and 1, 2, 4, and 8 h. Blood samples were immediately washed from the micropipettes with 0.75 ml of borate buffer into 0.25 ml of carrier DNA solution containing 250 μ g of unlabeled DNA, and 1.0 ml cold 10% TCA was added. The samples were centrifuged at 2,500 g for 20 min at 4°C, the supernate was removed, and the precipitate and supernate were counted in an automatic, well-type gamma counter (Searle Diagnostics Inc., DesPlaines, Ill.). In some animals, 100 μ l of blood was drawn into heparin-coated micropipettes at 1, 5, and 10 min and then centrifuged. 50 μ l of plasma was used for electrophoresis as described above, to estimate the size of the DNA remaining in circulation.

1 min before sacrifice, some animals were injected with 0.1 ml of rabbit IgG, iodinated with ¹³¹I as a plasma volume marker. These animals were killed by exsanguination through the renal artery and the organs, blood, and carcasses were counted for calculation of organ uptake (see below).

Serum and urine were obtained from some animals 30 min after injection. These samples were loaded onto a DEAE Sephadex A-25 column (Pharmacia Fine Chemicals) at 4°C, and equilibrated with 0.01 M Tris HCl at pH 7.2. The column was washed with 50–60 ml of starting buffer and then linear gradient elution was performed up to 1 M NaCl. Calibration using carrier free ¹²⁵I (New England Nuclear, Boston, Mass.) and iododeoxycytidine (Sigma Chemical Co.) showed that the iododeoxycytidine eluted in the wash, and ¹²⁵I was eluted at 0.6–0.7 M NaCl.

In Vitro Nuclease Assay

EXONUCLEASE. Blood, obtained from noninjected animals by cardiac puncture, was immediately spun in a chilled, siliconized tube, and the plasma was removed. ssDNA was added to fresh plasma, whole blood, or PBS at the concentration attained in vivo for a mouse receiving a 100- μ g dose of ssDNA. This was calculated to be 1 μ g ssDNA/20 μ l of blood or 1 μ g ssDNA/10 μ l plasma, assuming a blood volume of 2 ml and a hematocrit of 50. Each sample was incubated at 37°C for 10 min in the presence of 0.01 M MgSO₄. In a parallel experiment performed to check for nuclease inhibitors, blood, plasma, or buffer was incubated with 1 μ g ssDNA in the presence of 70 μ g DNase II (Sigma Chemical Co.) and MgSO₄. After incubation, 250 μ g of cold carrier DNA and 1.0 ml of 10% TCA was added, samples were centrifuged for 20 min at 2,500 g, and the precipitate and supernate were counted. Results were expressed as the percentage of counts in the soluble fraction over the total counts. Each sample contained 50,000–60,000 cpm to minimize counting error.

ENDONUCLEASE. To assess the in vitro effect of plasma on degradation of precipitable ssDNA, plasma obtained from noninjected animals was mixed with the starting ssDNA preparation and incubated at 37°C for 1, 10, and 30 min. The reaction was arrested by cooling on ice, and the size of the ssDNA was determined by polyacrylamide gel electrophoresis as described above.

Analysis of Data. Immediately before each experiment, a sample of the ssDNA to be injected was counted and a specific activity in cpm/ μ g was determined. Using this specific activity, counts remaining in the 10% TCA precipitate, supernate, and whole blood (precipitate plus supernate) were converted to μ g of DNA remaining/ml, and the concentration versus time data were plotted on semilogarithmic paper. Clearance velocities were calculated using the formula: $V = 2.3026 K S_0$, where S_0 and K are the y-intercept and slope, respectively, of the line obtained by linear regression analysis of the early data points as presented under Results. Since the clearance kinetics were nonlinear functions, curve analysis was also carried out using the PDP-10 MLAB program (26) for a nonlinear regression analysis (Division of Computer Research and Technology, National Institutes of Health, Bethesda, Md.). Least squares test fits were determined for a Michaelis-Menten kinetics model, the closest possible estimations for maximum

velocity (V_m) and Michaelis-Menten constant (K_m) were obtained, and clearance curves were simulated using these parameter estimates.

Production velocity of TCA-soluble label was analyzed according to the formula: $V = 2.3026 K S_0$, where K and S_0 were the slope and y-intercept of the line derived from linear regression analysis of the first seven data points. This extrapolated S_0 for soluble material was found to closely approximate the number of micrograms of soluble label in the initial preinjected preparation (1–1.5% of injected dose).

Specific organ uptake was determined by calculating ^{131}I and ^{125}I counts per minute for each organ, and for 100 μl of blood at the time of sacrifice. The ^{131}I counts per minute per organ divided by the ^{131}I counts per minute per milliliter of blood yielded the total milliliters of blood per organ. When both isotopes were present in a specimen, the ^{125}I counts were corrected for the Compton scatter of ^{131}I . Specific organ uptake was calculated as follows:

$$\text{specific uptake} = \left(\frac{^{125}\text{I cpm}}{\text{organ}} \right) - \left(\frac{^{131}\text{I cpm/organ}}{^{131}\text{I cpm/ml of blood}} \right) \times ^{125}\text{I cpm/ml of blood.}$$

Since the specific activity of the DNA was known, the μg DNA uptake per organ could be calculated (27).

Results

Disappearance Kinetics of Injected DNA. The whole blood disappearance curve of a 2- μg dose of ^{125}I -ssDNA (Figure 1A) showed an initial rapid exponential phase during which 90% of the administered dose was removed. A second, slower component was also evident with an increase in whole blood radioactivity at 30 min. This late increase in radioactivity was observed with all administered doses of ssDNA. Since it was thought that this late component might be a result of the production of breakdown products, whole blood samples were precipitated with 10% TCA, and the soluble (mononucleotide or free iodine) and precipitable (polynucleotide) fractions were analyzed separately. In this way, most breakdown products were excluded from analysis of disappearance curves. The clearance curves of the TCA-precipitable ssDNA showed a rapid initial clearance phase without a late increase in whole blood radioactivity. A second, slow or exponential component, representing 1.5–2% of the total injected material, was present in the TCA-precipitable DNA curves. Attempts to isolate and to characterize this persistent precipitable DNA by gel filtration and acrylamide electrophoresis showed that it was <1,000 daltons mol wt, and was not protein bound. Furthermore, when free ^{125}I , a known TCA-soluble material, was added to whole blood and precipitated with 10% TCA, as was done routinely in animal experiments, 8–10% of the label became trapped in the precipitate. Therefore, the TCA-precipitable DNA curves were analyzed by subtracting 10% of the soluble counts at a given time from the precipitable counts at that same time to correct for the counts entrapped in the precipitate. Analysis of the disappearance curves in this manner almost completely eliminated the slow component and showed the disappearance curves of TCA-precipitable ssDNA to be a rapid, exponential function (Fig. 1B).

Effect of Varying Dosage on Disappearance Kinetics. The clearance kinetics of TCA-precipitable ssDNA were examined after the administration of 2, 10, 50, 100, and 500 μg of ssDNA. As shown in Fig. 2, the rate of ssDNA clearance was not linearly related to dose, but clearance became saturated with increasing doses of ssDNA. In addition, the clearance velocity for any given dose was not constant,

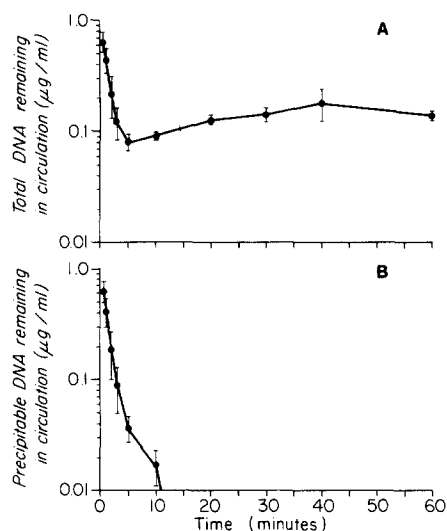


FIG. 1. Disappearance curves of ssDNA from circulation of mice. (A), the remaining whole blood radioactivity after administration of $2 \mu\text{g}$ ssDNA was converted to μg DNA/ml by the formula: $\text{DNA } \mu\text{g/ml} = \text{cpm per } 20 \mu\text{l sample} \times 50/\text{cpm per } \mu\text{g DNA}$. Each data point represents the mean \pm SD of at least five mice. An initial rapid phase of disappearance from blood is present, and then the amount of DNA remaining increases. (B), the amount of ssDNA precipitable with 10% TCA remaining in circulation is plotted for the same mice as in (A). The blood disappearance of TCA-precipitable ssDNA is described by a single rapid exponential function.

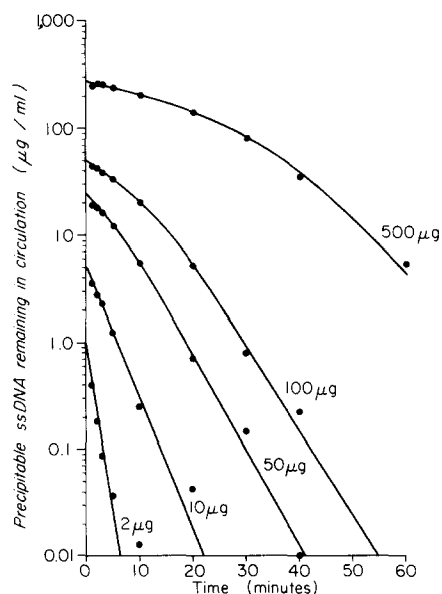


FIG. 2. Observed data points and computer-simulated precipitable ssDNA clearance curves based on estimated parameters (V_m and K_m) for each administered dose. Each (●) represents the mean observed value at each measured time point. The applicability of the Michaelis-Menten model to the data is evident from the close agreement of curves.

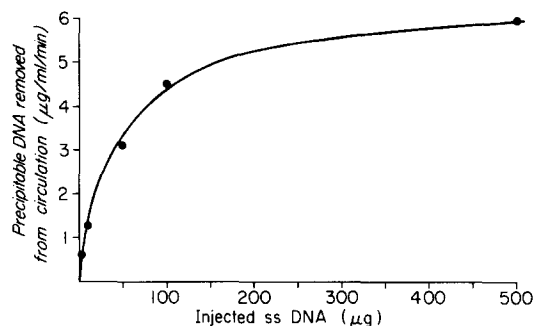


FIG. 3. Clearance kinetics of TCA-precipitable ssDNA. Clearance velocities ($\mu\text{g/ml/min}$) were calculated using linear regression analysis of early data points (see text), and they reach a maximum with higher doses.

but changed with the concentration of ssDNA in circulation at any given time as reflected by the changing slopes of the curves, particularly with higher doses. This behavior was consistent with a saturable, Michaelis-Menten clearance mechanism (28, 29, 30). Accordingly, clearance velocities were calculated using data from 30 s to 5 min for the 2, 10, and 50 μg doses, and from 30 s to 10 min for the higher doses (Materials and Methods). A dose-versus-clearance velocity curve yielded an approximate V_m of 6 $\mu\text{g/ml/min}$ and a K_m of 35 $\mu\text{g/ml}$ (Fig. 3). However, since clearance velocity for any given dose changed with time, as illustrated in Fig. 2, considerably different velocities could be generated for each dose by including more or fewer data points in the linear regression analysis. Therefore, the data were fit to the Michaelis-Menten equation ($dC/dt = -V_m C / (K_m + C)$, where C = concentration, and t = time) by the method of least squares by the MLAB computer program and V_m and K_m were generated for each dose. Using these parameter estimates, the computer simulated the clearance curves which were described by the Michaelis-Menten equation. A high degree of agreement of the data with the Michaelis-Menten model was found, as indicated in Fig. 2 by the close superposition of observed data points and the curves predicted by the model. No systematic deviations from the model were apparent at either end of the curves.

Organ Uptake of Injected DNA. Specific organ uptake in the liver, spleen, kidneys, lung, and skin was studied at 3, 20, and 60 min. As reported previously (17, 18, 20), the liver was by far the major organ of uptake, with 94.5% of the 2 μg -dose present in the liver at 20 min, and 8% at 60 min. At higher doses, however, the amount of radioactivity in the liver remained constant or actually increased over time. The larger the dose of ssDNA injected, the longer the liver continued to accumulate the radiolabeled material. This accumulation of radioactivity over time suggested to us either re-uptake of breakdown products or storage of material. To determine the role of the various organs in removal kinetics, organ uptake was examined at 3 min, a time when minimal reuptake or storage of radioactivity can be assumed. Fig. 4 shows the hepatic uptake curve and the removal of ssDNA from blood at 3 min at different doses. The liver accounted for $\approx 90\%$ of DNA removal at 3 min at all doses.

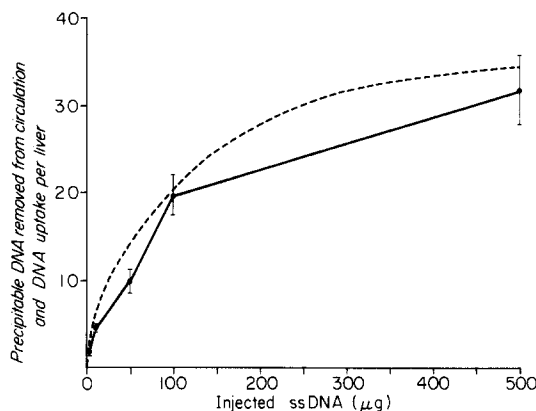


FIG. 4. Specific liver uptake (—) of ssDNA in mice sacrificed 3 min after injection of DNA. Each point represents the mean \pm SD for 3–4 mice. (---) represents the amount of precipitable ssDNA removed from circulation in the first 3 min after injection, based on the curves shown in Fig. 2. Hepatic uptake accounts for $\cong 90\%$ of the ssDNA removed from circulation at all doses.

Renal uptake represented only 2–5% of the total ssDNA removed from the circulation, and did not increase with increasing the dose. Whether this renal uptake represents only soluble breakdown products in the tubules or larger DNA at other sites within the kidney is currently under investigation. Splenic uptake played only a small role in ssDNA removal. However, as the liver became saturated with higher doses of DNA, splenic uptake appeared to increase from 2.2% of the DNA removed with a 2- μ g dose to 7% of the DNA removed with a 500- μ g dose. Lung and skin tissues showed negligible (<1% of the removed DNA) uptake at all examined time points (3, 20, 60 min).

Appearance of TCA-Soluble Material. The appearance of TCA-soluble material in the circulation was studied. Immediate production of soluble breakdown products was observed with no lag phase (Fig. 5). Significantly more TCA-soluble material was present in the circulation at 2 min than in the starting preparation (1–2% of starting preparation was soluble). Production increased to a peak at 30–40 min and then declined gradually. For comparison, the generation of TCA-soluble breakdown products was also examined with immune complexes consisting of human serum albumin and antibodies to human serum albumin, material known to be cleared from circulation by the hepatic mononuclear phagocyte system (Kupffer cells) (27). These curves showed a 40–60 min lag before any increase was demonstrable in circulating soluble products.

The velocity of production of TCA-soluble material at different doses of ssDNA was calculated using data points from 30 s to 10 min. A plot of dose-versus-production velocity showed that the velocity approached a maximum of 0.2 μ g/ml/min with a K_m of 130. These values are obviously inaccurate, however, since they will be greatly affected by cellular reuptake and urinary excretion of breakdown products. Indeed, urinary excretion of breakdown products, although not quantitated, was rapid. Radioactivity was detectable in the urine in significant amounts at 10 min.

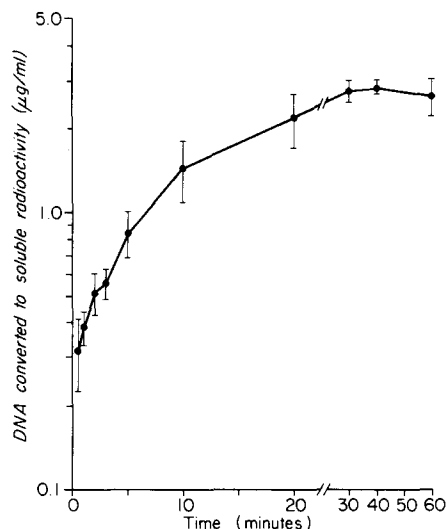


FIG. 5. Amount of TCA-soluble ssDNA present in the circulation after administration of 50 μg of ssDNA. Each point represents the mean \pm SD of at least five mice. μg of soluble ssDNA/ml were calculated using the specific activity in cpm/ μg of the injected preparation (as in Fig. 1). Immediate production of breakdown products is evident without a lag phase.

To demonstrate that the above measured soluble radioactivity actually represented ssDNA breakdown products, serum and urine obtained 30 min after injection were passed over ion exchange columns. 50–60% of serum radioactivity was shown to be iododeoxycytidine and the remainder was free iodine or dinucleotides. Only 30% of the ^{125}I label in the urine could be identified as iododeoxycytidine; most of the urinary soluble products were free ^{125}I .

Serum Nuclease Activity. To examine if the rapid appearance of soluble products was the result of a circulating plasma factor, fresh plasma was assayed *in vitro* for exonuclease activity. ssDNA was added to plasma at the same concentration as was present *in vivo* in mice receiving a 100- μg dose. Table I shows that no plasma exonuclease activity was demonstrable at 10 min, a time at which significant breakdown of ssDNA was evident *in vivo*. The activity of a commercial DNase was not inhibited by the addition of even large amounts of plasma, indicating that no exonuclease inhibitors were present in plasma which might have blocked ssDNA breakdown in the *in vitro* assay.

Characterization of Precipitable DNA Remaining in Circulation. In addition to the cleavage of soluble products from the DNA molecule by exonucleases, large precipitable DNA is cleaved into smaller fragments by endonucleases. To characterize the size of circulating ssDNA, plasma obtained at 1, 5, and 10 min after injection of 20 μg of ssDNA was characterized by electrophoresis on a 3.5% polyacrylamide gel. A rapid decrease in size of the DNA occurred (Fig. 6), with a reduction to approximately one-half of the starting molecular weight of the DNA at 1 min. At 10 min, the ssDNA remaining in circulation was cleaved to 80–120 nucleotide fragments (25,000–35,000 mol wt), roughly one-sixth the size of the injected preparation. The 1-min sample and controls with ssDNA

TABLE I
The Generation of TCA-Soluble ssDNA Products by Whole Blood, Plasma, and DNase In Vitro

Digestion mixture*	No DNase added		DNase added	
	n‡	Soluble radioactivity§	n	Soluble radioactivity
		%		%
ssDNA + PBS	8	2.63 ± 0.96¶	5	69.53 ± 1.72
ssDNA + blood	12	1.87 ± 0.29	7	71.31 ± 1.74
ssDNA + plasma	10	2.20 ± 0.45	5	72.28 ± 0.83

* 1 μ g Pool II ssDNA added to 20 μ l 0.01 M PBS pH 7.2, 20 μ l whole blood, or 10 μ l fresh plasma, and incubated with 0.01 M $MgSO_4$ at 37°C for 10 min. 250 μ g carrier DNA was added and the mixture was precipitated with cold 10% TCA.

‡ n, number of samples tested. Each sample was done in duplicate, and no more than two blood or plasma samples were obtained from any individual mouse.

§ Percent radioactivity equals cpm supernate/cpm precipitate + cpm supernate, expressed as the mean \pm 1 SD.

|| Commercial DNase added as a positive control (see text).

¶ No significant differences within the "DNase" and "No DNase" groups were observed.

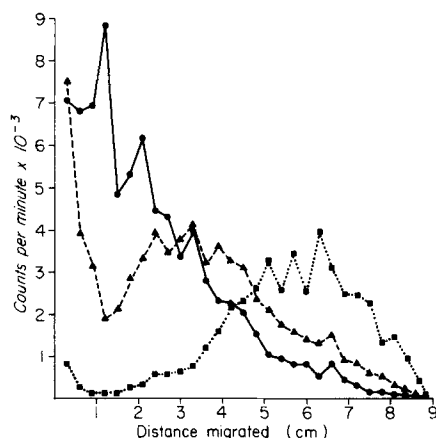


FIG. 6. Migration of radiolabeled ssDNA on polyacrylamide gel electrophoresis. (\blacktriangle) indicates the radioactivity in 50 μ l of plasma obtained at 1 min, and (\blacksquare), in 50 μ l of plasma obtained 5 min after injection of 20 μ g of ssDNA. (\bullet) represents the electrophoresis pattern of a mixture in vitro of 0.5 μ g ssDNA and 50 μ l normal plasma. Assuming a 2-ml blood volume for a 20-g mouse, this represents the theoretical concentrations of ssDNA in plasma at time 0. Electrophoresis was performed on 3.5% polyacrylamide slabs in 0.09 M Tris borate, 2.5 M EDTA buffer pH 8.2 at 10 V/cm for 2 h. 3-mm slices were cut, counted for ^{125}I radioactivity, and plotted as distance migrated from the well. Bromophenol blue and xylene cyanol migrated 6.2 and 3.1 cm, respectively, under these conditions, and were used for approximate molecular weight calculations (25) (Table II).

added to fresh plasma showed a large amount of material remaining near the well, suggesting possible interaction of DNA with serum proteins. It is of note that at later times, as the DNA was broken down to smaller sizes, less protein binding occurred. Analysis of the amount of ssDNA remaining in different size ranges showed an increase in the absolute amount of small nucleotides with

TABLE II
Size of Precipitable ssDNA Remaining in Circulation

Time after injection	Size of DNA (nucleotides)*			
	>500	250-500	100-250	<100
<i>min</i>			μg	
0‡	11.26 \pm 1.70§	5.83 \pm 0.69	2.34 \pm 0.88	0.56 \pm 0.17
1	4.80 \pm 0.15	4.99 \pm 0.01	4.68 \pm 0.42	1.93 \pm 0.64
5	0.38 \pm 0.05	0.93 \pm 0.01	4.52 \pm 0.15	3.25 \pm 1.30
10	0.25 \pm 0.01	0.48 \pm 0.09	0.85 \pm 0.25	1.62 \pm 0.58

* Based on PAGE of samples using the standard curves of Maniatis et al. (25) for ϕ X174 ssDNA.

‡ ssDNA mixed with fresh plasma in vitro and immediately subjected to polyacrylamide gel electrophoresis.

§ Mean (μg) \pm 1 SD based on two experiments, after administration of 20 μg of ssDNA.

time (Table II), indicating cleavage of ssDNA rather than the mere selective removal of larger molecules.

To determine if this rapid cleavage could be attributed to a circulating enzyme, ssDNA was incubated with fresh plasma without anticoagulants, or with heparinized plasma at 37°C for 30 min. Electrophoresis of these samples showed a definite decrease in size of the ssDNA after incubation with either heparinized or unanticoagulated plasma. Data were insufficient to allow for accurate quantitative comparisons with in vivo breakdown. However, it appeared that some, but not all of the endonuclease activity observed in vivo could be attributed to circulating enzymes.

Discussion

Previous studies have shown that administered DNA is rapidly removed from the circulation by the liver, and phagocytosis by the Kupffer cells was suggested as the mechanism responsible for this. Because of the known saturability of the mononuclear phagocyte system with a number of substances, it seemed pertinent to examine whether or not this held true for DNA as well.

This study has therefore attempted to define the behavior and clearance mechanisms of exogenously administered ssDNA over a wide range of doses. The work of Chused et al. (18), Dorsch et al. (20) and Tsumita and Iwanaga (17) was confirmed by showing that ssDNA was rapidly removed from the circulation and that the major organ of removal was the liver. When the clearance of total radioactivity was followed over time (Fig. 1 A), there was a late rise in circulating label at 30-40 min. This increase was the result of the appearance of TCA-soluble breakdown products in the circulation, and a large portion of those breakdown products could be identified as iododeoxycytidine, a mononucleotide. Breakdown products were rapidly excreted in the urine as either free ^{125}I or ^{125}I -deoxycytidine.

When these breakdown products were excluded from curve analysis, the clearance mechanism for ssDNA was clearly saturable (Figs. 2 and 3) and the kinetics closely fit a Michaelis-Menten clearance model. This model, although originally described for simple enzyme systems, has been applied to the mononuclear phagocyte system by Normann (28), and to in vivo clearance of

diphenylhydantoin (30) and ethanol (31) by Sedman et al. Computer-simulated curves based on this model (29, 30) for other substances looked remarkably similar to the whole blood disappearance curves for ssDNA shown in Fig. 2. We therefore applied our data to the Michaelis-Menten equation and obtained a high degree of agreement (Fig. 2). The mean values of the computer estimates for V_m and K_m were $7.2 \pm 1.4 \mu\text{g/ml/min}$ and $36.5 \pm 14.0 \mu\text{g/ml}$, respectively. These values agreed quite well with the V_m of $6.0 \mu\text{g/ml/min}$ and K_m of $35 \mu\text{g/ml}$, determined by simple dose-versus-clearance velocity graphing (Fig. 3). The usual concept of half life is not valid in describing nonlinear data such as this, since the rate of clearance is constantly changing over time (32). To further describe this system, we chose to measure the time taken for removal of 90% of the administered dose. At low doses such as the $2\text{-}\mu\text{g}$ dose used in previous studies (18, 20), 90% of the administered dose was removed at 3 min. However, since the removal mechanism was saturable, precipitable ssDNA persisted in the circulation considerably longer at higher doses. Removal of 90% of the $100\text{-}\mu\text{g}$ dose took 20 min, and removal of the $500\text{-}\mu\text{g}$ dose took 41 min.

The organ uptake data confirmed previous work (17, 18, 20), showing that the liver was the major organ for removal of circulating ssDNA. Furthermore, liver uptake was saturable in parallel with whole blood clearance (Fig. 4), suggesting that precipitable ssDNA clearance was mediated by binding to liver cells, and that as liver uptake mechanisms became saturated, clearance became saturated. Renal uptake represented 2-5% of the removal mechanism and did not alter with the alteration of the dose administered. Splenic uptake, however, increased in relative importance as the liver became saturated, suggesting a possible overflow or safety-valve role for the spleen in clearance, even if relatively small in comparison to hepatic uptake.

The possible role of antibodies to ssDNA must be considered in the rapid hepatic uptake of this material, since Thoburn et al. (32a) demonstrated that 44% of 7- to 12-mo-old C57Bl/6J mice had endogenous antibodies to ssDNA. Potentially, exogenous ssDNA could combine with antibodies and be removed by the mononuclear phagocyte system as large lattice immune complexes. However, the removal of ssDNA occurred 25-30 times faster than the removal of an equal dose of preformed immune complexes (27). Furthermore, as discussed below, phagocytosis of immune complexes is characterized by a lag in the appearance of breakdown products in the circulation, a phenomenon which was not seen with ssDNA. Finally, when ssDNA binding was measured by Farr assay in sera of eleven 3- to 4-mo-old C57Bl/6J mice, we found no antibodies to ssDNA. Therefore, we conclude that the clearance of ssDNA described in this study is not dependent upon immune complex formation, but is a function of the ssDNA itself.

The saturability of organ uptake and of clearance of ssDNA may be relevant to the finding of high levels of circulating ssDNA in patients after hemodialysis of trauma, or in those with SLE. Potentially, if a large bolus of ssDNA were released into the circulation, such as might occur after tissue injury or sunburn, clearance mechanisms could become saturated, enabling large molecular weight ssDNA to persist in circulation. Moreover, if the removal mechanism was susceptible to saturation with other materials such as immune complexes,

ssDNA might also remain in circulation longer than normal. Increased amounts of ssDNA might then be available for combination with antibodies to form immune complexes, for local deposition in tissues, or for presentation to immunocompetent cells. It is important to note that we could find no increased renal deposition of ssDNA at high doses, but that splenic uptake did increase slightly. To discover whether or not this splenic uptake is important in terms of increased antigen presentation to immunocompetent cells would be an intriguing study. However, the localization and molecular weight of the DNA within organs must be defined before any conclusions can be drawn.

This study also enabled us to make some statements about ssDNA degradation in vivo and the size of ssDNA which persisted in circulation. DNA is broken down in biological systems by two groups of enzymes; exonucleases and endonucleases (33). Exonucleases attack the ends of polynucleotide chains, yielding mononucleotides which are soluble in 10% TCA. Endonucleases attack linkages within the polynucleotide chain yielding shorter fragments, but they cannot degrade these fragments to soluble (mononucleotide) residues. One or both of these enzymes could potentially act: (a) intracellularly, after phagocytosis or membrane transport of the ssDNA molecule into a cell, (b) within the circulation, or (c) at the cell surface (membrane-bound enzyme).

Exonuclease activity was measured by the appearance of TCA-soluble ¹²⁵I label in the circulation. If exonucleases were intracellular and required prior phagocytosis of ssDNA, one would expect a lag phase of at least 6–30 min before the appearance of breakdown products in the circulation. This has been shown by Palmer et al. (34, 35) using colloidal human serum albumin, and by Moore et al. (36) using bovine serum albumin. With ssDNA, there was no lag phase, and there was a significant increase in soluble label by 2 min, reaching a peak at 30 min, the time at which breakdown products from a phagocytic process are just beginning to appear (Fig. 5). This strongly suggested that the exonuclease was not intracellular and did not depend upon prior phagocytosis, but was either a circulating or a membrane-bound enzyme. However, as shown in Table I, we were unable to show any significant plasma exonuclease activity. Since a number of studies (37, 38) have reported masking to serum nuclease activity by inhibitors released from cells during clotting, we used carefully prepared fresh plasma without anticoagulants. We also checked for plasma exonuclease inhibitors by adding plasma to a commercial enzyme of known activity. We were unable to show inhibitors which might have been masking exonuclease activity. This suggested that the exonuclease system may be a membrane-bound enzyme. Since such a large amount of the injected DNA went to the liver, this is potentially the location of this enzyme. It is well known (39–41) that the liver is rich in nucleases and that 5' nucleotidase, an exonuclease, is a liver membrane-bound glycoprotein (39).

If liver uptake in our system were simply a matter of binding of substrate (precipitable ssDNA) to enzyme with release of product (soluble mononucleotide), one would expect a close relationship between saturability curves of DNA clearance, liver uptake, and soluble product released. As discussed above, this was true of the DNA clearance and liver uptake curves. However, the curve of soluble product released versus dose, although saturable, showed a

130- $\mu\text{g/ml}$ K_m and a 0.2- $\mu\text{g/ml/minute}$ V_m . The difference between this V_m and the V_m for liver uptake can be explained on the basis of the rapid renal excretion of breakdown products, but the large difference between the two K_m is hard to explain. A renal threshold, enabling soluble products at high doses to persist in circulation, or cellular reuptake of nucleotides, which in itself is saturable, could both account for the increased K_m . However, we do not have enough data at this time to explain this value. Although we are confident that the exonuclease activity resides in the liver and is probably not dependent upon phagocytosis, we cannot conclude that ssDNA binds directly to this enzyme with subsequent release of mononucleotides.

Previous work has demonstrated that DNA is a good inducer of *in vitro* pinocytosis in macrophages (42). Furthermore, when daunorubicin, a drug which alone readily diffuses into tumor cells, was complexed with DNA, daunorubicin entry into cells was slowed, and it localized in lysosomes (43). This indirect evidence for the *in vitro* phagocytosis of DNA forms the basis for its use in the design of lysosomotropic drugs, as proposed by de Duve et al. (44). We could not find data, however, on the *in vivo* phagocytosis of DNA or on the *in vivo* breakdown of DNA in lysosomes. The absence of a lag phase in the appearance of soluble DNA breakdown products in the circulation appears inconsistent with the concept of phagocytosis and intralysosomal breakdown of ssDNA. Direct evidence on the cellular site of DNA breakdown is currently being sought.

Endonuclease activity was measured in our model by the decrease in size of the precipitable ssDNA, as measured by polyacrylamide gel electrophoresis (PAGE). Chused et al. (18), using sucrose density gradients, showed a decrease in size of DNA at 30 min. We have shown (Fig. 6), using the more sensitive PAGE system, that precipitable DNA was rapidly cleaved, with a marked reduction in size at 1 min (Table II). Since there was an absolute increase in the amount of smaller fragments, this could not be accounted for by selective removal of large ssDNA. Furthermore, in preliminary studies we demonstrated some of this activity in plasma *in vitro*. Although we certainly cannot rule out a role of tissue endonucleases as well, some of the endonuclease activity appeared to reside in a circulating enzyme. We do not yet have data on the saturability of this enzyme, nor on the size of its final breakdown product. More homogenous DNA preparations will be necessary to answer these questions. However, in our *in vivo* studies, many of the polynucleotide fragments were 100 nucleotides or less, corresponding to a mol wt of $\approx 20,000$ – $30,000$. The antigenicity and immunogenicity of polynucleotides this size are not well defined, and will require further investigation. However, these fragments could potentially pass through the glomerular basement membrane and lodge in the subepithelial area to combine locally with antibodies. It is of interest that the binding of ssDNA to glomerular basement membrane preparations and the local formation of immune complexes with antibodies to DNA has been demonstrated *in vitro* by Izui et al. (45).

In conclusion, we have presented evidence which suggests that injected ssDNA is rapidly removed and degraded *in vivo* by two enzyme systems acting simultaneously. Large molecular weight ssDNA is cleaved into smaller frag-

ments by a circulating endonuclease. These fragments (as well as the original DNA) are bound to the liver where they are attacked by what appears to be a membrane-associated exonuclease which cleaves off mononucleotides. This exonuclease system is saturable, so that with increasing doses of ssDNA administered, more polynucleotide fragments persist in the circulation and are available for attack by endonucleases. The fate of these persistent polynucleotide fragments and their potential role in formation of immune complexes, in induction of an immune response, or in local deposition in tissues is not yet clear. However, the behavior of these fragments, as well as the existence of factors which might alter DNA clearance and lead to their persistence, seem pertinent to our understanding of human and murine SLE.

Summary

Clearance of exogenous ssDNA from circulation was rapid and occurred primarily through the liver. With higher doses of single-stranded DNA (ssDNA), both liver uptake and whole blood clearance approached a maximum, enabling larger amounts of ssDNA to persist in the circulation. The large molecular weight material (precipitable ssDNA) which remained in circulation was rapidly cleaved to 20,000–30,000 mol wt fragments by endonucleases, at least some of which could be demonstrated in plasma *in vitro*. Mononucleotide breakdown products appeared rapidly in circulation with no lag phase, suggesting that exonuclease activity was not dependent upon prior phagocytosis. Since no exonuclease activity could be demonstrated in plasma *in vitro*, it was postulated that breakdown of ssDNA by exonucleases occurs on the surface of hepatocytes or Kupffer cells.

We wish to thank Ms. Trish Fadling for her excellent technical assistance.

Received for publication 17 October 1977.

References

1. Winfield, J. B., D. Koffler, and H. G. Kunkel. 1975. Role of DNA-anti-DNA complexes in the immunopathogenesis of tissue injury in systemic lupus erythematosus. *Scand. J. Rheumatol. Suppl.* 11:59.
2. Tan, E. M., P. H. Schur, R. I. Carr, and H. G. Kunkel. 1966. Deoxyribonucleic acid (DNA) and antibodies to DNA in the serum of patients with systemic lupus erythematosus. *J. Clin. Invest.* 45:1732.
3. Andres, G. A., L. Accinni, S. M. Beiser, C. L. Christian, G. A. Cinotti, B. F. Erlanger, K. C. Hsu, and B. C. Seegal. 1970. Localization of fluorescein-labeled antinucleoside antibodies in glomeruli of patients with active systemic lupus erythematosus nephritis. *J. Clin. Invest.* 49:2106.
4. Krishnan, C., and M. H. Kaplan. 1967. Immunopathologic studies of systemic lupus erythematosus. II. Antinuclear reaction of γ -globulin eluted from homogenates and isolated glomeruli of kidneys from patients with lupus nephritis. *J. Clin. Invest.* 46:569.
5. Koffler, D., P. H. Schur, and H. G. Kunkel. 1968. Immunological studies concerning the nephritis of systemic lupus erythematosus. *J. Exp. Med.* 126:607.
6. Fournie, G. J., S. Izui, P. H. Lambert, and J. J. Conte. 1977. Genesis and pathogenicity of anti-DNA antibodies. *Adv. Nephrol.* 6:47.

7. Beck, J. S., C. L. Oakley, and N. R. Powell. 1966. Transplacental passage of antinuclear antibody. *Arch. Dermatol.* 93:656.
8. Ward, J. R., R. S. Cloud, and L. M. Turner. 1964. Non-cytotoxicity of "nuclear antibodies" from lupus erythematosus sera in tissue culture. *Ann. Rheum. Dis.* 23:381.
9. Koffler, D., V. Agnello, R. Winchester, and H. G. Kunkel. 1973. The occurrence of single stranded DNA in the serum of patients with systemic lupus erythematosus and other diseases. *J. Clin. Invest.* 52:198.
10. Koffler, D., V. Agnello, and H. G. Kunkel. 1974. Polynucleotide immune complexes in serum and glomeruli of patients with systemic lupus erythematosus. *Am. J. Pathol.* 74:109.
11. Hughes, G. R. V., S. A. Cohen, R. W. Lightfoot, Jr., J. I. Meltzer, and C. L. Christian. 1971. The release of DNA into serum and synovial fluid. *Arthritis Rheum.* 14:259.
12. Tan, E. M. 1970. Production of potentially antigenic DNA in cells. In Sixth International Symposium on Immunopathology. P. A. Miescher, editor. Schwabe & Co., Basel, Switzerland. 346.
13. Gabrielsen, A. E. 1974. Lupus erythematosus: a disease of DNA discard? *Lancet.* II:1116.
14. Ledoux, L. 1965. Uptake of DNA by living cells. In Progress in Nucleic Acid Research and Molecular Biology. J. N. Davidson and W. E. Cohn, editors. Academic Press Inc., New York. 6:231.
15. Gosse, C., J. B. LePecq, P. Defrance, and C. Paoletti. 1965. Initial degradation of deoxyribonucleic acid after injection in mammals. *Cancer Res.* 25:877.
16. Paoletti, C., C. Gosse, and J. B. LePecq. 1963. Breakdown of desoxyribonucleic acid injected intravenously into rabbits: effect of plasma desoxyribonucleases. *Biochemistry (Engl. Transl. Biokhimiya)* 28:531.
17. Tsumita, T., and M. Iwanaga. 1963. Fate of injected deoxyribonucleic acid in mice. *Nature (Lond.)*. 198:1088.
18. Chused, T. M., A. D. Steinberg, and N. Talal. 1972. The clearance and localization of nucleic acids by New Zealand and normal mice. *Clin. Exp. Immunol.* 12:465.
19. Natali, P. G., and E. M. Tan. 1972. Experimental renal disease induced by DNA-anti DNA immune complexes. *J. Clin. Invest.* 51:345.
20. Dorsch, C. A., D. Chia, L. Levy, and E. V. Barnett. 1975. Persistence of DNA in the circulation of immunized rabbits. *Rheumatology.* 212:161.
21. Chia, D., C. Dorsch, E. V. Barnett, and L. Levy. 1977. Metabolism of exogenous single stranded DNA in normal and NZB/W mice. *Immunology.* 32:351.
22. Paetkau, V., and L. Langman. 1975. A quantitative batch hydroxyapatite method for analyzing native and denatured DNA at room temperature. *Anal. Biochem.* 65:525.
23. Bernardi, G. 1969. Chromatography of nucleic acids on hydroxyapatite. II. Chromatography of denatured DNA. *Biochim. Biophys. Acta.* 174:435.
24. Commerford, S. L. 1971. Iodination of nucleic acids *in vitro*. *Biochemistry.* 10:1993.
25. Maniatis, T., A. Jeffrey, and H. van deSande. 1975. Chain length determination of small double- and single-stranded DNA molecules by polyacrylamide gel electrophoresis. *Biochemistry.* 14:3787.
26. Knott, G. D., and D. K. Reece. 1972. MLAB: A civilized curve-fitting system. Proceedings of the Online '72 International Conference. Brunel University, England. 1:497.
27. Haakenstad, A. O., and M. Mannik. 1974. Saturation of the reticuloendothelial system with soluble immune complexes. *J. Immunol.* 112:1939.

28. Normann, S. J. 1974. Kinetics of phagocytosis. II. Analysis of *in vivo* clearance with demonstration of competitive inhibition between similar and dissimilar foreign particles. *Lab. Invest.* 31:161.
29. Hallberg, D., and A. McLean. 1973. The simulation of the elimination process for a substance injected into the blood stream. *Acta Med. Scand.* 194:173.
30. Gerber, N., and J. G. Wagner. 1972. Explanation of dose-dependent decline of diphenylhydantoin plasma levels by fitting to the integrated form of the Michaelis-Menten equation. *Res. Commun. Chem. Pathol. Pharmacol.* 3:455.
31. Sedman, A. J., P. K. Wilkinson, E. Sakmar, D. J. Weidler, and J. G. Wagner. 1976. Food effects on absorption and metabolism of alcohol. *J. Stud. Alcohol.* 37:1197.
32. Wagner, J. G. 1973. Properties of the Michaelis-Menten equation and its integrated form which are useful in pharmacokinetics. *J. Pharmacokinetic. Biopharm.* 1:103.
- 32a. Thoburn, R., D. Koffler, and H. G. Kunkel. 1971. Distribution of antibodies to native DNA, single-stranded DNA, and double-stranded RNA in mouse serums. *Proc. Soc. Exp. Biol. Med.* 136:711.
33. Lehninger, A. L. 1975. *Biochemistry, the Molecular Basis of Structure and Function.* Worth Publishers Inc., New York. 323.
34. Palmer, D. L., D. Rifkind, and D. W. Brown. 1971. ¹³¹I-labelled colloidal human serum albumin in the study of reticuloendothelial system function. II. Phagocytosis and catabolism of a test colloid in normal subjects. *J. Infect. Dis.* 123:457.
35. Palmer, D. L., D. Rifkind, and D. W. Brown. 1971. ¹³¹I-labelled colloidal human serum albumin in the study of reticuloendothelial system function. III. Phagocytosis and catabolism compared in normal, leukemic, and immunosuppressed human subjects. *J. Infect. Dis.* 123:465.
36. Moore, A. T., K. E. Williams, and J. B. Lloyd. 1977. The effect of chemical treatments of albumin and orosomucoid on rate of clearance from the rat bloodstream and rate of pinocytotic capture by rat yolk sac cultured *in vitro*. *Biochem. J.* 164:607.
37. Herriott, R. M., J. H. Connolly, and S. Gupta. 1961. Blood nucleases and infectious viral nucleic acids. *Nature (Lond.)* 189:817.
38. Frost, P. G., and P. J. Lachmann. 1968. The relationship of desoxyribonuclease inhibitor levels in human sera to the occurrence of antinuclear antibodies. *Clin. Exp. Immunol.* 3:447.
39. Gurd, J. W., and W. H. Evans. 1974. Distribution of liver plasma membrane 5' nucleotidase as indicated by its reaction with anti-plasma membrane serum. *Arch. Biochem. Biophys.* 164:305.
40. Aronson, N. N., and A. Yannarell. 1975. Effects of membrane ribonuclease and 3' nucleotidase on the digestion of polyuridylic acid by rat liver plasma membrane. *Biochem. Biophys. Acta.* 413:135.
41. Bartholeyns, J., C. Peeters-Joris, H. Reyckler, and P. Baudhiun. 1975. Hepatic nucleases: methods for the specific determination and characterization in rat liver. *Eur. J. Biochem.* 57:205.
42. Cohn, Z. A., and E. Parks. 1967. The regulation of pinocytosis in mouse macrophages. II. Factors inducing vesicle formation. *J. Exp. Med.* 125:213.
43. Trouet, A., D. D. Campeneere, and C. de Duve. 1972. Chemotherapy through lysosomes with a DNA-daunorubicin complex. *Nat. New Biol.* 239:110.
44. de Duve, C., T. de Barsey, B. Poole, A. Trouet, P. Tulkens, and F. Van Hoof. 1974. Lysosomotropic agents. *Biochem. Pharmacol.* 23:2495.
45. Izui, S., P-H. Lambert, and P. A. Miescher. 1976. In vitro demonstration of a particular affinity of glomerular basement membrane and collagen for DNA. *J. Exp. Med.* 144:428.